

## Exciton Localization in a Pt–Acetylide Complex

Enrique R. Batista\* and Richard L. Martin

Los Alamos National Laboratory, Theoretical Division, MS B268, Los Alamos, New Mexico 87545

Received: June 10, 2005; In Final Form: August 29, 2005

We present a theoretical study of the low-lying electronic excitations in the  $[\text{Pt}(\text{P}^n\text{Bu}_3)_2(\text{ethynylbenzene})_2]$  molecule. Although the ground electronic state possesses  $D_{2h}$  symmetry, with both ethynylbenzene ligands being equivalent, in the excited state the molecule breaks the symmetry deforming along a  $b_{3u}$  direction and localizing the excitation on a single ligand. This localized exciton is of  ${}^3\pi\pi^*$  nature with the unpaired electron and hole spread over one of the benzene rings and the ethyne linkage. The localization indicates an activated hopping mechanism for transport. Our estimate of the barrier is  $\sim 0.61$  eV.

### 1. Introduction

The set of materials based on platinum-acetylide  $\pi$ -conjugated oligomers has prompted great interest in recent years for their potential applications in highly efficient organic electroluminescent devices.<sup>1–4</sup> In these compounds the  $\pi$ -orbitals of the ligands are conjugated with the d orbitals of the Pt, allowing for charge migration along the oligomers. Electroluminescence in these materials might also be expected to be reasonably efficient, as the presence of the metal and the consequent spin–orbit coupling would allow both singlet and triplet electron–hole pairs to recombine emissively, an option not available to purely organic polymers due to the strong enforcement of spin selection rules in the light atoms.

Recent experimental work has been dedicated to understanding the spatial extent of the excited states.<sup>3,5</sup> Liu et al.<sup>6</sup> studied the absorption and photoluminescence spectra of the Pt–acetylide oligomers shown in Figure 1 with  $n = 1–5, 7$ . They found evidence for localization of the triplet excitation  $T_1$ , but delocalization of the lowest excited singlet  $S_1$ . Emmert et al.<sup>7</sup> studied the symmetry properties of the ground state and lowest excited triplet states of the  $[\text{Pt}(\text{P}^n\text{Bu}_3)_2(\text{ethynylbenzene})_2]$  (Figure 1 with  $n = 1$ ) via time-resolved infrared (TRIR) spectroscopy. They concluded that the symmetry of this basic monomer is reduced in the excited state from  $D_{2h}$  to  $C_{2v}$ , implying that only one of the two ligands participates in the electronic excitation. It was proposed that the reduction of symmetry is due to a displacement along the antisymmetric  $b_{3u}$  vibration involving the acetylenic unit.<sup>7</sup> We reported preliminary quantum chemistry calculations earlier,<sup>8</sup> which corroborated this localized excitonic model put forward by Emmert et al.

In this paper we report more fully on our computational study. The calculations confirm that in the lowest triplet excited state the molecule deforms along a  $b_{3u}$  coordinate, breaking the symmetry and localizing the excitation on one side. This (and subsequent calculations not reported here) gives additional evidence for localization of excitations in longer polymers and suggests that the charge migration occurs via activated hopping. The hopping barrier for the Pt monomer was calculated to be 0.61 eV.

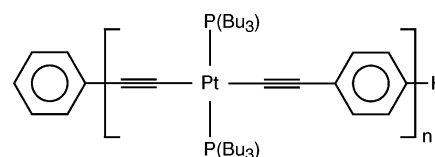


Figure 1. Scheme of the Pt–acetylide oligomers.

### II. Computational Methods

The electronic ground states of all the molecules presented in this work were calculated using B3LYP<sup>9,10</sup> density functional theory. The basis set used for the nonmetal atoms (H, C, O, and P) was a double- $\zeta$  basis with polarization functions, 6-31G\*. For the metal ions (Pt), the basis set was also double- $\zeta$ , LANL2DZ. This basis set was used in combination with a relativistic effective core potential (RECP)<sup>11</sup> that replaced the inner core electrons leaving the 5s, 5p, 5d, and 6s valence electrons in the calculation. The geometry of the molecules was optimized without symmetry constraints. The excited states were studied via density functional response theory (TDDFT)<sup>12–15</sup> and DFT- $\Delta$ SCF (difference in total energies between self-consistent calculation of the ground state and the lowest triplet state). In TDDFT typically the lowest 6 singlet and 6 triplet roots were obtained. All the calculations of the electronic structure of the molecules under study and geometry optimizations were performed using the Gaussian03<sup>16</sup> Rev. B.04 suite of codes for quantum chemistry.

### III. Results

The ground state of the  $[\text{Pt}(\text{P}^n\text{Bu}_3)_2(\text{ethynylbenzene})_2]$  molecule is a singlet. The geometry of the molecule is almost  $S_2$  symmetric at the Pt atom and  $D_{2h}$  if the butyl ligands are ignored. At the optimal geometry the benzene rings were found to be coplanar and perpendicular to the P–Pt–P axis (see Figure 2). The bond length of the ethyne linkage is 1.229 Å. The HOMO and LUMO orbitals have already been shown by Emmert et al.<sup>7</sup> to be  $\pi$  orbitals totally delocalized over the whole molecule with a small component of a platinum  $d_\pi$  orbital. Due to the symmetry of the molecule, the HOMO–1 and LUMO+1 look very much like the HOMO and LUMO, respectively, but differing in relative phase between the two sides of the molecule.

The vertical excitations from the ground state were calculated via TDDFT. The first excited state, at 3.06 eV, has the natural

\* To whom correspondence should be addressed. E-mail: erb@lanl.gov.

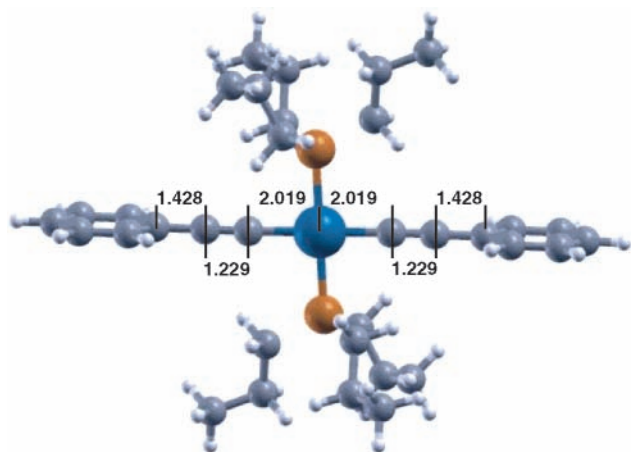


**Figure 2.** Geometry of the  $[\text{Pt}(\text{P}(\text{t})\text{Bu})_3]_2(\text{ethynylbenzene})_2$  molecule at the ground state.

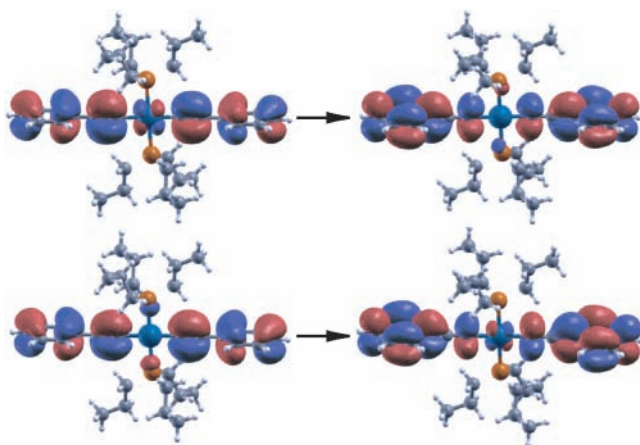


**Figure 3.** First vertical excitation from the ground state of  $[\text{Pt}(\text{P}(\text{t})\text{Bu})_3]_2(\text{ethynylbenzene})_2$ . Natural transition orbitals of the hole (left) and electron (right) pair. This first excitation consists mainly of the two excitations shown in this figure, with 59% probability of  $\phi_g \rightarrow \phi_u^*$  and 32% probability  $\phi_u \rightarrow \phi_g^*$ .

**TABLE 1: TD-DFT Energies of the Lowest Excitations of  $[\text{Pt}(\text{P}(\text{t})\text{Bu})_3]_2(\text{ethynylbenzene})_2$  at the Optimal Geometry of the Ground State**

mult	energy	type
T	3.06	$^3\pi\pi^*$
T	3.10	$^3\pi\pi^*$
T	3.76	$^3\text{LMCT}$
T	3.89	$^3\text{LMCT}$
S	3.99	$^1\text{LMCT}$
T	4.03	
T	4.07	$^3\pi\pi^*$
S	4.12	$^1\pi\pi^*$
S	4.16	$^1\text{LMCT}$
S	4.18	
S	4.26	
S	4.29	

transition orbital (NTOs)<sup>8,17</sup> representation shown in Figure 3. Notice that the two orbitals on the left ( $\pi$  orbitals) are identical except for the inversion parity about the Pt atom. The top orbital ( $\phi_g$ ) is the *gerade* orbital and the lower one ( $\phi_u$ ) is *ungerade*. The opposite is true for the orbitals on the right column ( $\pi^*$  orbitals,  $\phi_u^*$  and  $\phi_g^*$ ), indicating that the first excitation is composed of two contributions  $\phi_g \rightarrow \phi_u^*$  and  $\phi_u \rightarrow \phi_g^*$  with 59 and 32% amplitude, respectively. The second excited triplet state is nearly degenerate with the first one, 0.04 eV higher (see Table 1), and involves the same NTOs but with single particle excitations  $\phi_u \rightarrow \phi_u^*$  and  $\phi_g \rightarrow \phi_g^*$ . Thus, the first state is

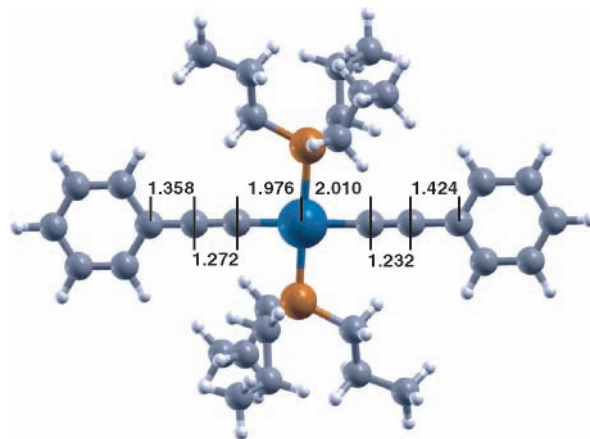


**Figure 4.** Geometry at the lowest triplet state.

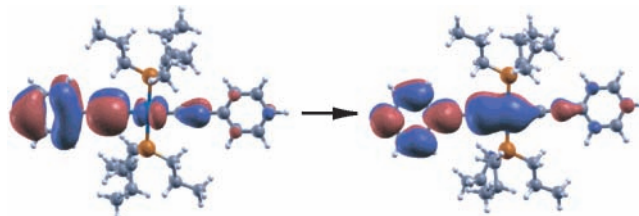


**Figure 5.** First excited state of  $[\text{Pt}(\text{P}(\text{t})\text{Bu})_3]_2(\text{ethynylbenzene})_2$  at the lowest triplet geometry. Natural transition orbitals of the hole (left) and electron (right) pair.

ungerade and the second *gerade*. At this symmetric geometry, the two cannot mix.

Although the triplet vertical excitations from the ground state are delocalized over the whole molecule, a very different picture is observed if one relaxes the geometry of the molecule in the excited state. The lowest triplet electronic state of  $[\text{Pt}(\text{P}(\text{t})\text{Bu})_3]_2(\text{ethynylbenzene})_2$  was calculated via unrestricted open shell SCF and its geometry optimized. The optimal geometry is shown in Figure 4. At its minimum the triplet state is stabilized by 0.61 eV relative to the vertical geometry. This decrease in energy comes from two factors: rearrangement of the charge density and a relaxation of the geometry. Figure 4 shows that at the triplet state the benzene rings have rotated by  $90^\circ$  relative to the ground state. Also, the  $\text{C}\equiv\text{C}$  bond on the left has become longer by 3.5% whereas on the opposite side the  $\text{C}\equiv\text{C}$  bond is almost unchanged. This change in conformation corresponds to a deformation along a  $b_{3u}$  mode of the  $D_{2h}$  symmetry group, previously discovered by Emmert et al.<sup>7</sup> The localization causes the  $\text{C}\equiv\text{C}$  bond on the left to become weaker, a “double bond”, and the one on the right remains a triple bond. This analysis is supported by the natural transition orbitals for the lowest excited state at the triplet minimum (see Figure 5), which show that the excited electron came from a  $\pi$  orbital localized on the left, leaving there a hole, and populates an antibonding  $\pi^*$  on the same side. A Mulliken population analysis of these two orbitals indicates that in the  $\pi$  orbital 37% of the hole is located at the  $\text{C}\equiv\text{C}$  bond, 47% is located on the benzene ring, 9% in the conjugated Pt d orbital, and the remaining 7% is on the right side of the molecule. In the  $\pi^*$  state the populations are similar, 23% in the  $\text{C}\equiv\text{C}$  bond, 56% on the ring and 11% on the Pt, but now predominantly in the appropriate p orbital.

To understand the origin of the localization, we performed TDDFT calculations to generate the energy landscape shown in Figure 6. The energy curves are schematic and based on the TDDFT excitation energies at the geometries of the ground singlet and triplet state. At the symmetric geometry, there are

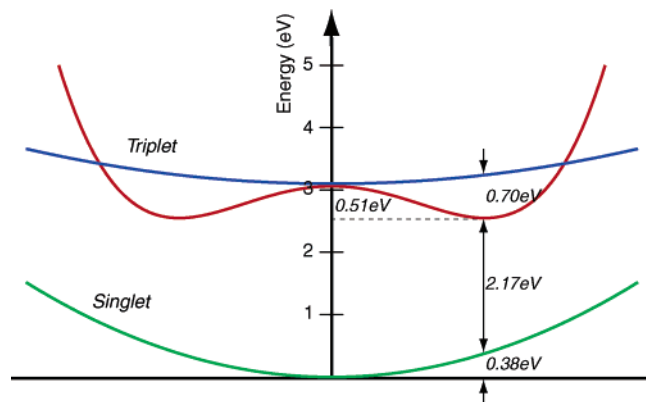


**Figure 6.** TDDFT energy landscape of the ground state and lowest triplets along the  $b_{3u}$  direction, which connects the singlet and triplet minima.

two nearly degenerate triplets, one ungerade and one gerade. Under a  $b_{3u}$  symmetry distortion, they mix to produce two localized states, one on each side of the molecule. At the minimum geometry for the triplet, its partner lies some 0.70 eV higher and corresponds to the excitation localized on the opposite side of the molecule; that is, the state in which the electronic excitation is “out of phase” with the nuclear distortion. The double well potential computed by TDDFT yields a barrier for exciton hopping of 0.51 eV, with the barrier occurring for the symmetric geometry. This is slightly lower than the estimate of 0.61 eV from unrestricted SCF.<sup>26</sup> The experimental emission energies for phosphorescence shown in ref 6 indicate a broad peak at 2.20 eV and a sharp feature at 2.40 eV. Measurements by Emmert et al.<sup>7</sup> indicate a very structured phosphorescence spectrum with peaks between 2.53 and 2.80 eV. Our calculated emission energy compares very well with experiment. The emission energy for the  $|0\rangle \rightarrow |0\rangle$  was calculated at 2.55 eV (see Figure 6), which after zero point energy corrections is 2.45 eV. The vertical emission energy was obtained at 2.17 eV.

The vibrational frequencies for the  $[\text{Pt}(\text{P}^t\text{Bu})_3]_2(\text{ethynylbenzene})_2$  molecule calculated at the triplet minimum yield a triple bond frequency (right side of Figure 4) of  $2152 \pm 70 \text{ cm}^{-1}$ , which is in good agreement with the TRIR spectrum by Emmert et al.<sup>7</sup> The error bar in the calculated frequency corresponds to the root-mean-square error calculated for the T-82F set of diatomic molecules, using B3LYP and the 6-31G\* basis set.<sup>18</sup> The vibrational frequency of the “double bond” associated with the exciton (left side of Figure 4) is calculated to be  $158 \text{ cm}^{-1}$  lower in frequency ( $1994 \pm 70 \text{ cm}^{-1}$ ) with an intensity 12 times weaker than that of the triple bond. This is in disagreement with the peak identified as the “double bond” in ref 7, which lies at  $1740 \text{ cm}^{-1}$ . We believe that the actual peak may be hidden in the background of the experimental spectrum. Note that though the frequency ( $1994 \text{ cm}^{-1}$ ) is considerably higher than expected for a double bond, only 37% of the hole resides there, according to the NTO analysis. A simple-minded calculation would indicate a shift of  $427 \text{ cm}^{-1}$  ( $158/0.37$ ) if the entire hole were localized in the “double bond”, which would place the peak at  $1725 \text{ cm}^{-1}$ , in the vibrational range expected for a C=C double bond.

By way of contrast, the lowest singlet excitation is delocalized at all geometries studied here (see Figure 7). Although the geometry of the lowest singlet excitation ( $S_1$ ) could not be optimized, we found that the electron–hole pair of  $S_1$  was delocalized over the whole molecule even at the geometry of the lowest triplet. This is also consistent with the conclusions of Liu et al.<sup>6</sup> of a delocalized singlet excitation based on the

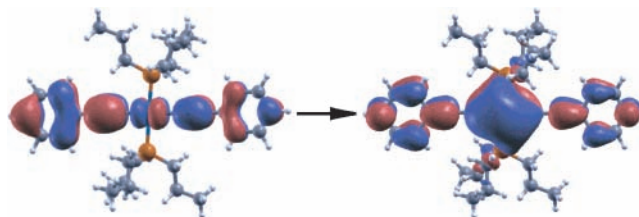


**Figure 7.** Natural transition orbitals of the lowest singlet excited state of  $[\text{Pt}(\text{P}^t\text{Bu})_3]_2(\text{ethynylbenzene})_2$  at the lowest triplet geometry. The NTOs show that the singlet excitation is delocalized over the whole molecule even at the optimal geometry of the triplet state, which has broken symmetry.

small singlet–triplet gap. The singlet excitation was calculated to be 1.09 eV above the energy of the lowest triplet, which is in good agreement with the experimental data of ref 6 where the singlet–triplet gap was estimated to be 1.36 eV on the basis of an extrapolation of the phosphorescence energy. Using the measurements of phosphorescence from ref 7, the singlet–triplet gap is between 1.27 and 1.00 eV, in good agreement with the calculated one.

In summary, we find that the lowest triplet state of  $[\text{Pt}(\text{P}^t\text{Bu})_3]_2(\text{ethynylbenzene})_2$  localizes on one of the ethynylbenzene linkages. This is in agreement with the TRIR spectroscopic results of Emmert et al.<sup>7</sup> In contrast, a recent DFT study of a similar complex, PE2, found the lowest triplet state to be delocalized over both ligands.<sup>19</sup> The primary difference in the calculations, aside from a slightly different ligand, is our use of hybrid DFT (B3LYP) versus the generalized gradient approximation (GGA,PW91)<sup>20,21</sup> used by Cooper et al. Recent research has focused on the problems conventional functionals (local-density approximation, LDA, and GGA) have in terms of overestimating delocalization effects. This manifests itself in many ways; one being the well-known tendency of the LDA to overbind molecules,<sup>18</sup> and another the fact that they predict metallic behavior in the class of materials known as Mott insulators.<sup>22–24</sup> Hybrid DFT largely remedies both these problems. Therefore, we suspect that the difference between the present results and those of Cooper et al., lies in the behavior of the GGA functional used by them. To test this, we repeated our calculations with the PW91 GGA, and find that within this approximation the triplet state remains delocalized. This is in contrast to both hybrid DFT and experiment and constitutes one more demonstration that pure functionals, LDA and GGA, lead to overestimates of delocalization in excited states.<sup>25</sup>

#### IV. Conclusions

We have reported a theoretical study of the localization of electronic excitations in  $[\text{Pt}(\text{P}^t\text{Bu})_3]_2(\text{ethynylbenzene})_2$ . At the vertical geometry, the electron–hole pair breaks the symmetry of the molecule through a distortion along a  $b_{3u}$  mode, in agreement with the original conclusions of Emmert et al. This deformation and localization is the result of two nearly degenerate excited states, one symmetric and the other anti-symmetric with respect to inversion. A small perturbation in the molecular geometry along a mode of  $b_{3u}$  symmetry, allows the two to mix and results in a double well potential. This is a particularly clean example of the second-order Jahn–Teller effect.

We will report our results on longer oligomers elsewhere, but suffice it to say that, as one would expect, we find similar localization behavior in the longer chains. We conclude that transport in these systems will be dominated by an activated



hopping. Our best estimate for the barrier in the monomer is 0.61 eV.<sup>26</sup>

**Acknowledgment.** This work was supported by the Division of Chemical Sciences, Office of Basic Energy Sciences, U.S. Department of Energy at Los Alamos National Laboratory. We thank James A. Brozik and Andrew P. Shreve for helpful discussions.

## References and Notes

- (1) Baldo, M. A.; O'Brien, D. F.; You, Y.; Shoustikov, A.; Sibley, S.; Thompson, M. E.; Forrest, S. R. *Nature* **1998**, *395*, 151.
- (2) Wilson, J. S.; Dhoot, A. S.; Seeley, A. J. A. B.; Khan, M. S.; Köhler, A.; Friend, R. H. *Nature* **2001**, *413*, 828.
- (3) Köhler, A.; Wilson, J. S.; Friend, R. H.; Al-Suti, M. K.; Khan, M. S.; Gerhard, A.; Bassler, H. *J. Chem. Phys.* **2002**, *116*, 9457.
- (4) Zhuravlev, F.; Gladysz, J. A. *Chem.-A Eur. J.* **2004**, *10* (24), 6510.
- (5) Jones, S. C.; Coropceanu, V.; Barlow, S.; Kinnibrugh, T.; Timofeeva, T.; Bredas, J.-L.; Marder, S. R. *J. A. Chem. Soc.* **2004**, *126*, 11782.
- (6) Liu, Y.; Jiang, S.; Glusac, K.; Powell, D. H.; Anderson, D. F.; Schanze, K. S. *J. A. Chem. Soc.* **2002**, *124*, 12412.
- (7) Emmert, L. A.; Choi, W.; Marshall, J. A.; Yang, J.; Meyer, A.; Brozik, J. A. *J. Phys. Chem. A* **2003**, *107*, 11340.
- (8) Batista, E. R.; Martin, R. L. Natural transition orbitals. In *Encyclopedia of Computational Chemistry*; von Ragu Schleyer, P., Allinger, N. L., Clark, T., Gasteiger, J., Kollman, P. A., Schaefer, H. F., III, Schreiner, P. R., Eds.; John Wiley & Sons Ltd.: Chichester, U.K., 2004.
- (9) Lee, C.; Yang, W.; Parr, R. G. *Phys. Rev. B* **1988**, *37*, 785.
- (10) Becke, A. D. *J. Chem. Phys.* **1993**, *98*, 5648.
- (11) Hay, P. J.; Wadt, W. R. *J. Chem. Phys.* **1985**, *82*, 299.
- (12) Jamorski, C.; Casida, M. E.; Salahub, D. R. *J. Chem. Phys.* **1996**, *104*, 5134.
- (13) Petersilka, M.; Grossmann, U. J.; Gross, E. K. U. *Phys. Rev. Lett.* **1996**, *76*, 1212.
- (14) Bauernschmitt, R.; Ahlrichs, R.; Hennrich, F. H.; Kappes, M. M. *J. A. Chem. Soc.* **1998**, *120*, 4439.
- (15) Casida, M. E. In *Recent Advances in Density Functional Methods*; Chong, D. P., Ed., World Scientific: Singapore, 1995; Vol. 1.
- (16) Frisch, M. J.; Trucks, G. W.; Schlegel, H. B.; Scuseria, G. E.; Robb, M. A.; Cheeseman, J. R.; Montgomery, J. A., Jr.; Vreven, T.; Kudin, K. N.; Burant, J. C.; Millam, J. M.; Iyengar, S. S.; Tomasi, J.; Barone, V.; Mennucci, B.; Cossi, M.; Scalmani, G.; Rega, N.; Petersson, G. A.; Nakatsuji, H.; Hada, M.; Ehara, M.; Toyota, K.; Fukuda, R.; Hasegawa, J.; Ishida, M.; Nakajima, T.; Honda, Y.; Kitao, O.; Nakai, H.; Klene, M.; Li, X.; Knox, J. E.; Hratchian, H. P.; Cross, J. B.; Adamo, C.; Jaramillo, J.; Gomperts, R.; Stratmann, R. E.; Yazyev, O.; Austin, A. J.; Cammi, R.; Pomelli, C.; Ochterski, J. W.; Ayala, P. Y.; Morokuma, K.; Voth, G. A.; Salvador, P.; Dannenberg, J. J.; Zakrzewski, V. G.; Dapprich, S.; Daniels, A. D.; Strain, M. C.; Farkas, O.; Malick, D. K.; Rabuck, A. D.; Raghavachari, K.; Foresman, J. B.; Ortiz, J. V.; Cui, Q.; Baboul, A. G.; Clifford, S.; Cioslowski, J.; Stefanov, B. B.; Liu, G.; Liashenko, A.; Piskorz, P.; Komaromi, I.; Martin, R. L.; Fox, D. J.; Keith, T.; Al-Laham, M. A.; Peng, C. Y.; Nanayakkara, A.; Challacombe, M.; Gill, P. M. W.; Johnson, B.; Chen, W.; Wong, M. W.; Gonzalez, C.; Pople, J. A. *Gaussian 03*, revision B.04; Gaussian, Inc.: Pittsburgh, PA, 2003.
- (17) Martin, R. L. *J. Chem. Phys.* **2003**, *118*, 4775.
- (18) Staroverov, V. N.; Scuseria, G. E.; Tao, J.; Perdew, J. P. *J. Chem. Phys.* **2003**, *119*, 12129.
- (19) Cooper, T. M.; Blaudeau, J.-P.; Hall, B. C.; Rogers, J. E.; McLean, D. G.; Liu, Y.; Toscano, J. P. *Chem. Phys. Lett.* **2004**, *400*, 239.
- (20) Perdew, J. P. Unified theory of exchange and correlation beyond the local density approximation; In *Electronic Structure of Solids '91*; Ziesche, P., Eschrig, H., Eds.; Akademie Verlag: Berlin, 1991; p 11.
- (21) Perdew, J. P.; Wang, Y. *Phys. Rev. B* **1992**, *45*, 13244.
- (22) Martin, R. L.; Illas, F. *Phys. Rev. Lett.* **1997**, *79* (8), 1539.
- (23) Moreira, I. D. R.; Illas, F.; Martin, R. L. *Phys. Rev. B* **2002**, *65* (15), 155102.
- (24) Kudin, K. N.; Scuseria, G. E.; Martin, R. L. *Phys. Rev. Lett.* **2002**, *89* (26), 266402.
- (25) Tretiak, S.; Igumenshchev, K.; Chernyak, V. *Phys. Rev. B* **2005**, *71* (3), 033201.
- (26) The zero-point energies for the ground state and lowest triplet states are 21.23 and 21.12 eV, respectively. For the triplet state at the ground-state geometry we obtained five negative frequencies, of average  $-174\text{ cm}^{-1}$ . The electronic state obtained from the  $\Delta$ SCF calculation is the diabatic one. Ignoring the negative frequencies the zero-point energy of this state is 21.01 eV. Including these zero-point corrections to the estimation of the barrier by unrestricted SCF, we obtain a barrier of 0.50 eV. The presence of multiple negative frequencies and the fact that the triplet eigenstate from  $\Delta$ SCF is localized makes this correction of uncertain value.